THE JOURNAL OF BIOLOGICAL CHEMISTRY VOL. 286, NO. 2, pp. 987–996, January 14, 2011

The Role of Heme and the Mitochondrion in the Chemical and Molecular Mechanisms of Mammalian Cell Death Induced by the Artemisinin Antimalarials*

Received for publication, May 18, 2010, and in revised form, October 5, 2010 Published, JBC Papers in Press, November 8, 2010, DOI 10.1074/jbc.M110.144188

Amy E. Mercer[‡1], **Ian M. Copple**[‡], **James L. Maggs**[‡], **Paul M. O'Neill**[§], **and B. Kevin Park**[‡]

From the [‡]*Medical Research Council Centre for Drug Safety Science and the* [§]*Department of Chemistry, The University of Liverpool, Liverpool L69 3GE, United Kingdom*

The artemisinin compounds are the frontline drugs for the treatment of drug-resistant malaria. They are selectively cytotoxic to mammalian cancer cell lines and have been implicated as neurotoxic and embryotoxic in animal studies. The endoperoxide functional group is both the pharmacophore and toxicophore, but the proposed chemical mechanisms and targets of cytotoxicity remain unclear. In this study we have used cell models and quantitative drug metabolite analysis to define the role of the mitochondrion and cellular heme in the chemical and molecular mechanisms of cell death induced by artemisinin compounds. HeLa ρ^0 cells, which are devoid of a functioning electron transport chain, were used to demonstrate that actively respiring mitochondria play an essential role in endoperoxide-induced cytotoxicity (artesunate IC_{50} values, 48 h: HeLa cells, 6 ± 3 μM; and HeLa ρ^0 cells, 34 ± 5 μM) via the generation of reactive oxygen species and the induction of mitochondrial dysfunction and apoptosis but do not have any role in the reductive activation of the endoperoxide to cytotoxic carbon-centered radicals. However, using chemical modulators of heme synthesis (succinylacetone and protoporphyrin IX) and cellular iron content (holotransferrin), we have demonstrated definitively that free or protein-bound heme is responsible for intracellular activation of the endoperoxide group and that this is the chemical basis of cytotoxicity (IC_{50} value and biomarker of bioactivation levels, respectively: 10β-(*p*-fluorophenoxy)dihydroartemisinin alone, 0.36 ± 0.20 μM and 11 ± 5%; and with succinylacetone, >100 μM and 2 ± 5%).

The endoperoxide antimalarials are a class of semi-synthetic compounds derived from the natural product artemisinin (**1**) (see Fig. 1) that are currently deployed in the frontline combination treatments for drug-resistant malaria because of their rapid clearance of parasites and high tolerability in humans (1, 2). Despite the widespread use of artemisinin-based compounds (ARTs)[2] (2), there have been persistent reports of neurotoxicity and embryotoxicity in cross-species animal studies, although this hazard has not translated to clinical use (2–5). It is currently perceived that the benefits of these drugs in treating malaria outweigh the risks when administered in the second and third trimesters of pregnancy; however, the World Health Organization have contraindicated the use of ARTs during the first trimester (6). The emergence of resistance to the ARTs is a pressing problem (7, 8), and the development of novel synthetic endoperoxides with improved efficacy and pharmacokinetics is therefore a priority area (9, 10). The major structural differences between the novel synthetic derivatives, resulting in increased systemic exposure, have the potential to induce highly variable toxicology and pharmacology (11). Therefore, the elucidation of the factors that define cell susceptibility to the ARTs is essential to facilitate the safe use of existing ARTs therapies; to inform the design of safe, novel, endoperoxide compounds in which pharmacological activity is dissociated from toxicological effects and to define the molecular target to enable their consideration and potential development as anticancer agents (12).

The endoperoxide group contained within the artemisinin (**1**) framework functions as both the pharmacophore and toxicophore. It is hypothesized that its one-electron reductive activation by an Fe(II) species to toxic carbon-centered radicals is essential for activity (Fig. 1) (13). The parasiticidal mechanism of action is not fully understood, and the chemical source of activation and the parasite target remain under investigation. However, it has been postulated that the endoperoxides have multiple targets including the parasite sarco/endoplasmic reticulum Ca^{2+}-ATPase, PfATP6, and heme- and non-heme-containing proteins while also inducing reactive oxygen species (ROS) and lipid peroxidation (13–16).

Our previous studies in mammalian cells have demonstrated that activation of the endoperoxide bridge to carbon-centered radicals only occurs in sensitive proliferating cells and not their primary counterparts and therefore that this differential activation is the chemical basis of selective cytotoxicity (17). The mechanism of endoperoxide-induced apoptotic cell death via ROS generation, mitochondrial membrane depolarization, caspase-3 and -7 activation, and DNA

* This work was supported in part by funds from the Medical Research Council (to A. E. M.) and the European Union (to I. M. C.) as part of the FP7 framework.

[1] To whom correspondence should be addressed: MRC Centre for Drug Safety Science, Sherrington Bldgs., The University of Liverpool, Liverpool L69 3GE, UK. Tel.: 44-151-7950382; Fax: 44-151-7945540; E-mail: aemercer@liv.ac.uk.

[2] The abbreviations used are: ART, artemisinin-based compound; PFDHA, 10β-(*p*-fluorophenoxy) dihydroartemisinin; ETC, electron transport chain; THF, terahydrofuran; SA, succinylacetone; PPIX, protoporphyrin IX; HTF, holotransferrin; MTT, 3-(4,5-dimethylthiazol-2-yl)-2,5-diphenyl-tetrazolium bromide; PI, propidium iodide; TMRE, tetramethylrhodamine ethyl ester; HBSS, Hanks' balanced salt solution; DCFH-DA, dichlorofluorscein diacetate; MRM, multiple-reaction monitoring; ROS, reactive oxygen species; MMP, mitochondrial membrane potential.

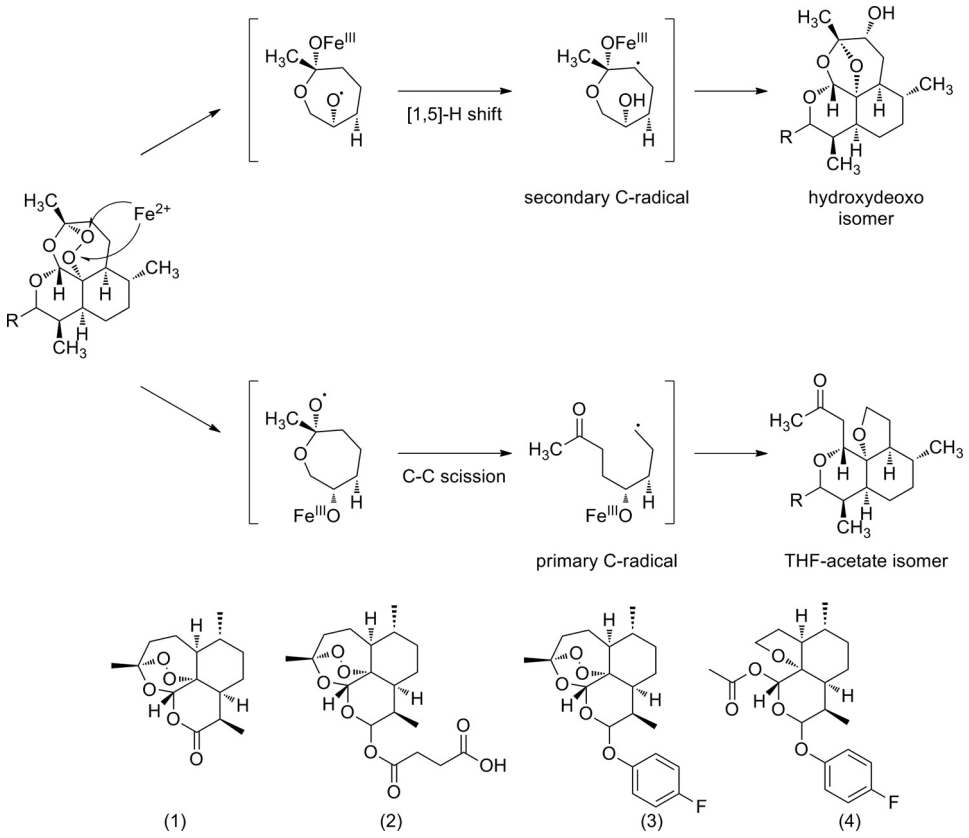

FIGURE 1. **The proposed mechanism of activation of the endoperoxide group in ART-derived compounds and structures of artemisinin (1), artesunate (2), PFDHA (3), and the THF acetate isomer of PFDHA (4).**

degradation has been well characterized in several cell types (17–19). Nevertheless, crucial information defining the primary cellular target of cytotoxicity and the exact intracellular mechanism of chemical activation remains unclear.

Intriguingly, the ARTs display a range of cytotoxic activity among mammalian cells (17, 18, 20). The iron activation hypothesis provides an explanation for this selectivity, proposing that cytotoxicity is dependent upon the higher concentration of iron required by malignant cells and neuronal cells to sustain continued growth and proliferation (21). Accordingly, sensitive cells have an increased number of transferrin receptors responsible for cellular iron uptake and higher intracellular iron levels, and pretreatment with iron chelators can reduce cytotoxicity (18, 19). In addition, recent biochemical evidence has been presented suggesting that heme may be a physiologically relevant mediator of the ARTs in cancer cells, and the authors have used biomimetic chemistry to speculate that this may be due to the formation of heme adducts (22).

Several investigations have implicated the mitochondrion in the antiparasitic (23, 24), cytotoxic (17), and embryotoxic (25, 26) mechanisms of action of the ARTs. Elegant studies performed with a yeast model and isolated mitochondria of parasite and mammalian cell origin have suggested that, in contrast to the iron activation theory, the mitochondrion may be a direct target and mediator of endoperoxide activity and further may underlie selectivity to the parasite (27, 28). The authors of these studies hypothesized that the mitochondria play a dual role: the electron transport chain (ETC) delivers reducing equivalents for activation of the endoperoxide function and, as a consequence, the mitochondria are damaged; ROS are generated leading to the eventual induction of parasite death.

In the present investigations, we have applied our established techniques to quantify bioactivation of the endoperoxide group via C-centered radicals and cell death *in vitro* to define more clearly the chemical and molecular mechanisms that determine mammalian cell susceptibility to the ARTs. Specifically we have defined the role of the ETC of the mitochondria, using ρ^0 cells that have been depleted of mitochondrial DNA, and that of heme, using chemical modulators of heme synthesis, in the chemical bioactivation of the endoperoxide group and the induction of cell death. The investigations were carried out using two endoperoxide compounds: artesunate (**2**), which is administered therapeutically as an antimalarial, and 10β-(*p*-fluorophenoxy)dihydroartemisinin (PFDHA) (**3**), an artemisinin derivative used as a chemical probe of endoperoxide-induced cell death because of its enhanced metabolic stability (17).

EXPERIMENTAL PROCEDURES

Materials—The human HeLa and HeLa ρ^0 cell lines were kindly supplied by Dr E. Bampton (Medical Research Council Toxicology Unit, Leicester, UK). HL-60 cells were purchased from European Collection of Cell Cultures (Salisbury, UK). The annexin V-FITC/propidium iodide (PI) staining kit was from Abd Serotec (Kidlington, Oxford, UK). Artesunate (**2**)

was kindly supplied by Dafra Pharma International (Belgium), PFDHA (**3**) was synthesized by the method of O'Neill *et al.* (29), and the tetrahydrofuran (THF)-acetate isomer of PFDHA (**4**) was prepared by an iron-catalyzed rearrangement (17). All other materials and chemicals were purchased from Sigma-Aldrich.

Cell Culture—HeLa and HeLa ρ^0 cell lines were maintained in DMEM high glucose medium supplemented with fetal bovine serum (10% v/v), L-glutamine (1% w/v), and sodium pyruvate, which was supplemented with uridine (50 μM) for HeLa ρ^0 cell culture. HL-60 cells were maintained in RPMI 1640 medium supplemented with fetal bovine serum (10% v/v) and L-glutamine (1% w/v). All of the cells were incubated under humidified air containing 5% CO_2 at 37 °C. Cell viability was above 95% for all of the experiments based on trypan blue exclusion (30). Drug stock solutions were made up in Me_2SO, and the final solvent concentration was below 0.5% (v/v) in each incubation.

Measurement of Cytotoxicity Using the 3-(4,5-Dimethylthiazol-2-yl)-2,5-diphenyl-tetrazolium Bromide (MTT) Assay and the Neutral Red Assay—HeLa/HeLa ρ^0 cells (5×10^3/well) were plated in triplicate in flat-bottomed 96-well plates and incubated for 24 h before exposure to each compound (0.005–100 μM). In experiments performed in the presence of modulators of heme synthesis, intracellular iron levels and antioxidants succinylacetone (SA, 0.5 mM), protoporphyrin IX (PPIX, 1 μM), holotransferrin (HTF, 10 μM), and tiron (1 mM) were added to the cells immediately prior to the addition of the drug. Cell viability was measured by the MTT (17) and neutral red (31) assays as described previously. All of the results are expressed as percentages of the values for vehicle-treated cells. The IC_{50} values were calculated from individual inhibition curves plotted by Grafit software (Erithacus, West Sussex, UK).

Flow Cytometric Measurement of Apoptotic and Necrotic Cells—Drug-treated cells were stained with annexin V and PI using a commercially available kit according to the manufacturer's instructions. A minimum of 5000 cells were analyzed by flow cytometry (Epics XL; Beckman Coulter, Buckinghamshire, UK). Annexin V-FITC fluorescence was measured on fluorescence channel 1, and PI fluorescence was measured on fluorescence channel 3. The proportions of viable cells (annexin-negative/PI-negative), apoptotic cells (annexin-positive/PI-negative), and necrotic/late apoptotic cells (annexin-positive/PI-positive) were calculated using WinMDI software (version 2.8; Scripps Institute).

Flow Cytometric Analysis of Mitochondrial Depolarization—Tetramethylrhodamine ethyl ester (TMRE) was used to identify cells with a high mitochondrial membrane potential (MMP) as described previously (17).

Flow Cytometric Analysis of ROS Generation—ROS generation was monitored using dichlorofluoroescein diacetate (DCFH-DA). Plated cells were pretreated with DCFH-DA (5 μM, 30 min), the dye solution was then removed, and the cells were washed twice in Hanks' balanced salt solution (HBSS) (1 ml) before drug was added. Following incubation, the cells were washed twice (HBSS, 1 ml) before resuspension (HBSS, 1 ml) and analysis by flow cytometry. A minimum of 5000 cells were analyzed, and the fluorescence intensity was measured using fluorescence channel 1. To correct for any fluorescence of the drug, duplicate samples were prepared without the addition of DCFH-DA for all incubations. In experiments performed in the presence of the antioxidant tiron, 1 mM tiron was added following incubation with DCFH-DA immediately prior to the addition of artesunate.

Determination of Cytochrome c Release by Western Blot—Drug-treated cells (2×10^5) were washed in ice-cold HBSS and resuspended in 50 μl of mitochondrial isolation buffer (250 mM sucrose, 20 mM HEPES, 5 mM $MgCl_2$, 10 mM KCl, pH 7.4) containing 0.05% digitonin. The cells were left on ice for 10 min before centrifugation (13,000 rpm, 3 min). The pellet was retained as the mitochondrially enriched fraction, and the supernatant was retained as the cytosol-containing fraction. Subsequently, both pellets and supernatants were analyzed by Western blotting for cytochrome *c* as described previously (32).

Determination of Caspases-3 and -7 Activities—A commercial caspase-glo 3/7 kit (Promega, Madison, WI) was used to measure the combined DEVD-ase activity of caspases-3 and -7. The assay provides a proluminescent caspase-3/7 substrate, which contains the tetrapeptide sequence DEVD, which is cleaved by the caspases to produce a luminescent signal. The kit was used according to the manufacturer's instructions, and the levels of luminescence were measured using a fluorescence microplate reader (BioTek FL600).

Determination of Cellular Heme Content—The method was based on the protocol of Sassa (33). To a pellet of endoperoxide-treated cells (1×10^5) was added an aqueous solution oxalic acid (500 μl, 2 M). The samples were shaken before heating (100 °C, 30 min). Standard solutions of hemin (0.01–10 mM) were prepared (water/methanol, MeOH 1:1, v/v containing 1% bovine serum albumin) and heated with oxalic acid, as above. The samples and standard solutions (200 μl) were plated into a white 96-well plate, and the fluorescence of the deferrated heme was measured (excitation, 400 nm; emission, 662 nm). The results were corrected for non-heme endogenous porphyrins by preparing cell blanks in oxalic acid without heating.

LC-MS/MS Analysis and Quantification of Intracellular Endoperoxide Bioactivation—Intracellular activation of the endoperoxides was monitored by LC-MS/MS. The instrument was an API 2000 triple-quadrupole mass spectrometer (AB Sciex, Warrington, UK) interfaced to a PerkinElmer Series 200 autosampler and a PerkinElmer pump. The data were collected and analyzed by the Analyst 1.3 software (AB Sciex). Cells (1 ml of 1.5×10^4 HeLa cells/ml or 4 ml of 1×10^6 HL-60 cells/ml) were incubated with PFDHA (**3**) (48 h for HeLa, 24 h for HL-60) at 37 °C. Following incubation, artesunate (**2**, 1 nmol) was added as an internal standard before the samples were prepared as described previously (17) and were analyzed by LC-MS/MS multiple reaction monitoring (MRM). Chromatographic separation was achieved on an Agilent ZORBAX Eclipse XDB-C8 column (150 × 3.9 mm inner diameter, 5 μm; Agilent Technologies, Santa Clara, CA). The mobile phase consisted of methanol with 10 mM aqueous ammonium acetate (70:30, v/v) delivered at a flow

TABLE 1

Analyte specific parameters and fragmentation transitions for tandem mass spectrometric analyses of artesunate (2), PFDHA (3), and PFDHA THF acetate (4)

Parameter	Artesunate (2)	PFDHA (3)	PFDHA THF acetate (4)
Fragmentation transition	402.1 to 163.1	396.0 to 163.0	396.0 to 266.7
Declustering potential (V)	21	6	21
Focusing potential (V)	370	370	370
Entrance potential (V)	12	8	5
Collision energy (V)	30	17	30
Collision cell entrance potential (V)	18.6	14	19
Collision cell exit potential (V)	26	10	14
Dwell time	200	200	100

rate of 0.4 ml/min. The mass spectrometer was operated in positive ion mode. The operating parameters were optimized via the quantitative optimization facility in Analyst software as follows: ion spray voltage of +5.0 kV, back pressures for the collision gas of 2 p.s.i., curtain gas of 20 p.s.i., nebulizer gas (GS1) of 30 p.s.i., and turbo gas (GS2) of 65 p.s.i.; the turbo gas temperature was 300 °C. Analyte-specific parameters and fragmentation transitions are detailed in Table 1. All of the gases used were nitrogen. Calibration curves of peak area *versus* analyte mass (5–5000 pmol) were generated from solutions of synthetic PFDHA, PFDHA THF acetate, and artesunate in methanol, and the limit of quantification was calculated to be 50 pmol using the method of least squares line fit. The efficiency of PFDHA and PFDHA THF acetate recovery was corrected for by the quantification of the internal standard, artesunate.

Statistical Analysis—The values are expressed as the means ± S.E. The data were analyzed for non-normality using a Shapiro-Wilk test. Student's *t* test was used when normality was indicated; a Mann-Whitney *U* test was used for nonparametric data. All of the calculations were performed using Stats Direct statistical software; the results were considered significant when the *p* values were less than 0.05.

RESULTS

Active Mitochondria Play an Important Role in the Induction of Apoptotic Cell Death via ROS Generation—The role of the activity of the mitochondrial ETC in ART-induced cell death was investigated using HeLa ρ^0 cells and their normal HeLa cell counterpart. HeLa ρ^0 cells have been depleted of mitochondrial DNA, which encodes the majority of the ETC. Therefore, they still contain mitochondria but lack a fully functional ETC and so utilize glycolysis instead of oxidative phosphorylation to generate ATP (34, 35). The cytotoxicity of PFDHA and artesunate (IC_{50} values) against HeLa and HeLa ρ^0 cells was determined using the MTT assay of total cellular dehydrogenase activity (36) and also by measuring the ability of viable cells to accumulate the cationic dye neutral red in the lysosomes via the maintenance of pH gradients through the production of ATP (31) (Table 2). The neutral red assay was included to confirm that any assessments of ART cytotoxicity made by the MTT assay of dehydrogenase activity were not affected by direct enzyme inhibition or the ETC status of the ρ^0 cells. The results demonstrate that the endoperoxide compounds are significantly more cytotoxic to the

TABLE 2

Cytotoxicity of the ARTs against HeLa and HeLa ρ^0 cells (48 h)

The IC_{50} values (μM) were derived from the MTT assay and neutral red assay and are expressed as the means ± S.D. calculated from the concentration-response curves of three independent experiments. ND, not determined. The *p* values indicate the significance of the IC_{50} values in HeLa cells compared with HeLa ρ^0 cells as tested by Student's *t* test for parametric data.

	MTT assay			NR assay		
	ρ^+	ρ^0	*p* value	ρ^+	ρ^0	*p* value
PFDHA	13 ± 4	92 ± 9	0.0012	15 ± 4	>100	ND
Artesunate	6 ± 3	34 ± 5	0.0114	16 ± 6	44 ± 9	0.0006

HeLa cells than the HeLa ρ^0 cells, with values three to seven times greater in cells without a functioning ETC.

The mechanism of cell death induced by artesunate was defined by measuring two diagnostic parameters. The annexin V/PI double staining method was used to identify apoptotic cells in which annexin V binds to the externalized phosphatidylserine residues (annexin-positive) and necrotic and late apoptotic cells in which concomitant PI staining of DNA occurs as a result of leaky cell membranes (annexin- and PI-positive) (Fig. 2*A*). These results show that in HeLa cells, artesunate induces significant levels of dose-dependent apoptosis, which progresses to low levels of late apoptosis/necrosis at higher concentrations (Fig. 2*B*). In contrast, in HeLa ρ^0 cells, death progresses predominantly via necrosis, with low levels of apoptosis apparent. For example, when treated with artesunate (50 μM, 48 h), HeLa cells are 54 ± 2% apoptotic and 24 ± 9% necrotic/late apoptotic, whereas HeLa ρ^0 cells are 21 ± 5% apoptotic and 67 ± 21% necrotic/late apoptotic.

The role of the mitochondria was further investigated by examining mitochondria membrane depolarization and the release of cytochrome *c* into the cytosol. TMRE was used to label cells with high mitochondrial membrane potential, and any reduction in fluorescence was attributed to MMP (Fig. 2*C*). Artesunate induced dose-dependent mitochondria membrane depolarization in HeLa cells, which reached a maximum of 71 ± 7% of cells (100 μM), but in HeLa ρ^0 the fraction of cells with depolarized mitochondrial membranes was lower, with significant levels only seen from 50 μM and a maximum of 49 ± 4% (100 μM) (Fig. 2*C*). The release of cytochrome *c* from the mitochondria into the cytosol is a hallmark of apoptosis (37) and was measured by immunoblot analysis of mitochondria and cytosol-containing fractions prepared from artesunate-treated cells (Fig. 2*D*). Artesunate induced a significant dose-dependent cytochrome *c* release in HeLa cells, which reached a maximum of 61 ± 4% of total cytochrome *c* released (48 h; Fig. 2*D*). Lower levels of cytochrome *c* release were evident in HeLa ρ^0 cells (maximum of 33 ± 17% release), and their response was also more variable (48 h). During the apoptotic pathway, the release of cytochrome *c* and the formation of the apoptosome trigger the activation of caspases-3 and-7, which are responsible for chromatin condensation and DNA fragmentation. The induction of caspase-3 and -7 activities by artesunate was measured using a luminescent assay (Fig. 2*E*). Artesunate induced a dose-dependent increase in activity at lower concentrations (1–10 μM, 48 h) in HeLa cells. However, the complete death of cells at high concentrations (100 μM) resulted in control levels of

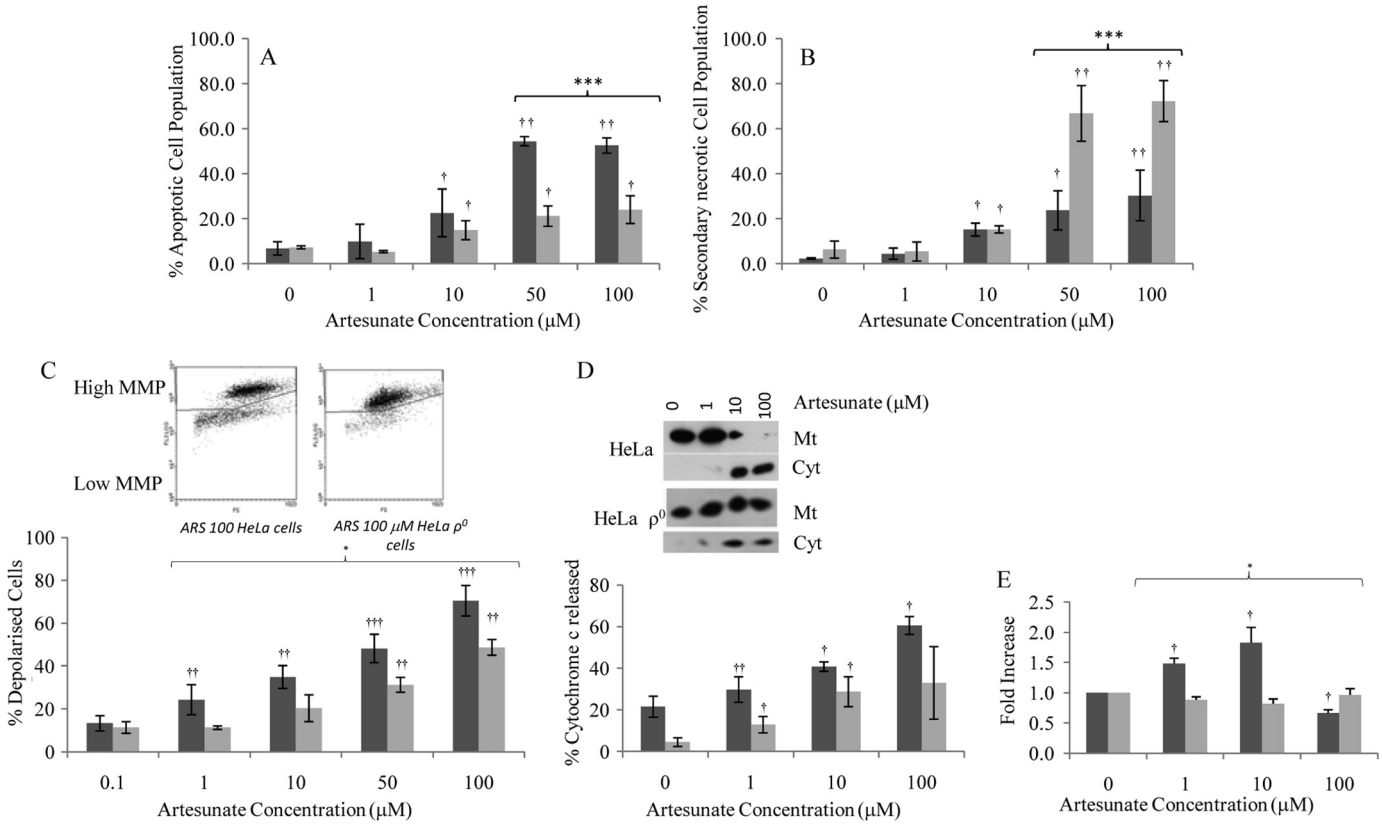

FIGURE 2. **Artesunate induces different mechanisms of cell death in HeLa and HeLa ρ^0 cells (48 h).** Following treatment with artesunate, the cells were dual-stained with annexin V and propidium iodide (manufacturer's instructions), and the levels of apoptosis and necrosis were measured by flow cytometry as described under "Experimental Procedures." *A* and *B*, concentration-dependent increases in apoptotic cells (stained with annexin V; *A*) and secondary necrotic/late apoptotic cells (stained with both annexin v and propidium iodide; *B*). *C*, artesunate induces concentration-dependent mitochondrial membrane depolarization. The cells were stained with TMRE (50 nM), and the MMP was measured by flow cytometry as described under "Experimental Procedures." Representative dot plots of TMRE-stained cells demonstrate TMRE accumulation in cells with high MMP (0 h) as high fluorescence (FL-2). Following treatment with artesunate (100 μM, 48 h), the cells with depolarized mitochondria have low MMP and reduced TMRE fluorescence. *D*, artesunate induces concentration-dependent release of cytochrome *c* in to the cytosol. Treated cells were processed as described under "Experimental Procedures." The mitochondria-containing fraction (*Mt*) and cytosol-containing supernatant (*Cyt*) were analyzed by Western blot for cytochrome *c* and actin. The gels were densitometrically scanned, and the amount of cytochrome *c* released into the cytosol was normalized to the amount of actin present; representative blots are shown. The amount of cytochrome *c* release was expressed as the percentage released into the cytosol of the total cytochrome *c* in both mitochondria and cytosol. *E*, artesunate induces concentration-dependent increases in caspases-3 and -7 activity in HeLa cells. The cells were assayed for caspase-3 and -7 activity using a commercially available kit as described under "Experimental Procedures." All of the results are the means ± S.E. of four independent sets of experiments. *Darker bars*, HeLa cells; *lighter bars*, HeLa ρ^0. †, $p < 0.05$; ††, $p < 0.01$; †††, $p < 0.001$ significance of artesunate-treated cell data compared with vehicle control. *, $p < 0.05$; **, $p < 0.01$; ***, $p < 0.001$ significance of HeLa data compared with HeLa ρ^0.

caspase activity. Conversely, no significant caspase-3/-7 activity was evident in HeLa ρ^0 cells (48 h).

The drug-induced generation of ROS was assessed by the pretreatment of cells with DCFH-DA. Esterase cleavage of the acetate groups forms dichlorodihydrofluorescein, which accumulates in the cells and undergoes oxidation by ROS to fluorescent dichlorofluorescin. The investigations of artesunate (100 μM) over a 48-h time course demonstrated that early maximal levels of ROS generation were attained at 16 h (2.3 ± 0.5-fold over control), which is much earlier than cytotoxicity is observed (Fig. 3*A*). In addition, ROS generation was reduced in HeLa ρ^0 cells (Fig. 3*A*). We have used tiron, a cell membrane-permeable superoxide scavenger (38) to define the link between ROS induction and the initiation of cell death. The results show that the addition of tiron significantly inhibits ROS generation at an early 24-h time point (Fig. 3*B*) and also inhibits the induction of cytotoxicity (48 h) (Fig. 3*C*).

The Activity of the Electron Transport Chain Plays No Role in the Chemical Activation of the Endoperoxide Group—The cellular bioactivation of the endoperoxide bridge was quantified using PFDHA (**3**, 10 μM; 48 h) as a chemical probe. A time-dependent loss of parent compound was accompanied by the formation of the THF acetate isomer (**4**), indicative of endoperoxide bridge activation via the primary carbon-centered radical (Fig. 1). Quantification of the parent compound and the THF acetate isomer revealed that maximum levels of activation were seen after 48 h of incubation: 61 ± 12 and 64 ± 13% of the parent compound remained in HeLa and HeLa ρ^0 cells (Fig. 4*A*), respectively, and 13 ± 2 and 12 ± 2% of the PFDHA had undergone activation through the radical species to form the isomer (Fig. 4*B*). There was no significant difference between the extents of bioactivation in the HeLa and HeLa ρ^0 cells.

Cellular Heme Is Essential for Endoperoxide-induced Cytotoxicity and the Chemical Activation of the Endoperoxide Group—The role of cellular heme was investigated in HL-60 cells because of their acute sensitivity to the ARTs (17). The cytotoxicity of artesunate and PFDHA was calculated (IC_{50} values) in the presence of modulators of heme synthesis and intracellular iron levels (Fig. 5) (39): SA (0.5 mM) inhibits

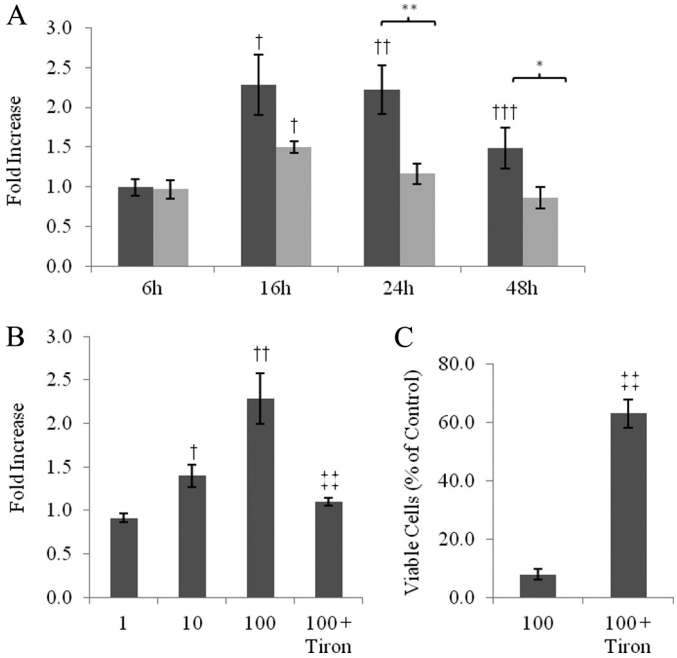

FIGURE 3. **Artesunate induces different levels ROS generation in HeLa and HeLa ρ^0 cells and cytotoxicity is dependent on ROS generation.** The cells were pretreated with DCFH-DA (5 μM, 30 min) before the addition of artesunate. Following drug incubation, ROS generation was measured by flow cytometry as described under "Experimental Procedures." *A*, time dependence of ROS generation induced by artesunate (100 μM). *B*, concentration dependence of ROS generation induced by artesunate and in the presence of tiron (1 mM) (24 h). *C*, the effect of the antioxidant tiron (1 mM) on cytotoxicity (24 h) measured by MTT assay as described under "Experimental Procedures." The results are the means ± S.E. of six independent sets of experiments. *Darker bars*, HeLa cells; *lighter bars*, HeLa ρ^0. †, $p < 0.05$; ††, $p < 0.01$; †††, $p < 0.001$ significance of artesunate-treated cell data compared with vehicle control. **, $p < 0.01$; ***, $p < 0.001$ significance of HeLa data compared with HeLa ρ^0. ‡‡, $p < 0.01$ significance of artesunate data compared with artesunate with tiron treatment.

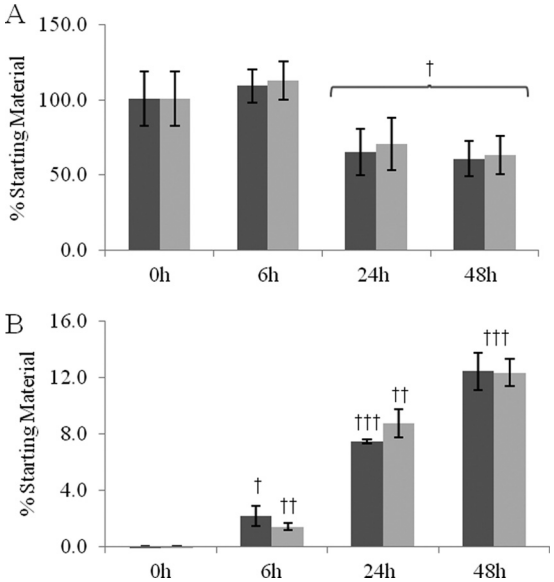

FIGURE 4. **PFDHA (3) is activated to PFDHA THF acetate (4) in HeLa and HeLa ρ^0 cells.** The cells were extracted following incubation with PFDHA (10 μM, 48 h), and the amounts of **3** and **4** present were assayed by LC-MS/MS-MRM, as described under "Experimental Procedures." *A*, time dependence of PFDHA disappearance. *B*, PFDHA THF acetate formation. *Darker bars*, HeLa cells; *lighter bars*, HeLa ρ^0. The results are the means ± S.D. of four independent sets of experiments. †, $p < 0.05$; ††, $p < 0.01$; †††, $p < 0.001$ significance of PFDHA-treated cell data compared with vehicle control.

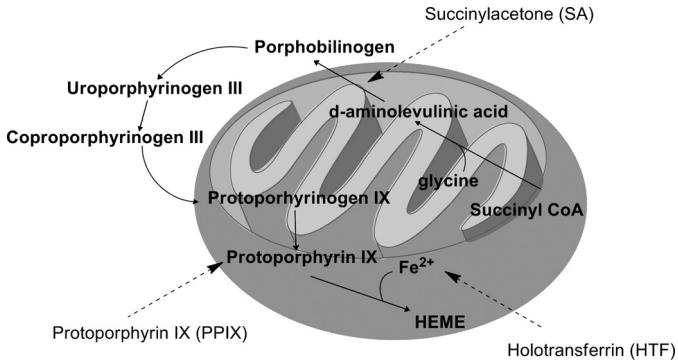

FIGURE 5. **A schematic representation of the effects of exogenous modulators on the heme biosynthetic pathway.**

δ-aminolevulinate dehydratase, PPIX (1 μM) is the immediate precursor to heme, and HTF (10 μM) was added as an exogenous source of cellular Fe(II). The heme content of the cells was also measured (Table 3). The results demonstrate that the addition of SA inhibits heme synthesis, evident by a significant reduction in cellular heme content, and abrogated significantly ART-induced cytotoxicity. The addition of PPIX increased heme synthesis to levels ~2.5 times greater than normal and increased sensitivity to ART-induced cytotoxicity significantly. The addition of HTF did not affect cellular heme content or ART-induced cytotoxicity significantly. When the modulators were added in combination, the presence of PPIX overcame the inhibition of heme synthesis induced by SA; cellular heme levels were measured that were significantly greater than control levels. The combination with PPIX also overcame SA-induced inhibition of cytotoxicity; IC_{50} levels were similar to those when cells were treated with endoperoxide alone. The addition of HTF with SA was also shown to overcome SA-induced inhibition of heme synthesis: cellular heme content was equivalent to control levels. However, cytotoxicity is only partially reversed; IC_{50} values are ~15–130 times higher than when cells are treated with ARTs alone.

The effect of these modulators upon the intracellular bioactivation of the endoperoxide bridge in HL-60 cells was characterized using PFDHA (1 μM; 24 h) (Fig. 6). PFDHA underwent bioactivation, demonstrated by a significant loss of parent compound (64 ± 5% of control levels) and formation of THF acetate biomarker (11 ± 5%). The addition of SA inhibited activation of PFDHA significantly: high levels of parent compound remained following 24 h of incubation (104 ± 16%), and correspondingly small amounts of the THF acetate biomarker (2 ± 5%) were produced. In the presence of PPIX, levels of bioactivation remained unchanged (62 ± 16% parent compound and 16 ± 10% THF acetate biomarker), whereas HTF increased turnover significantly (39 ± 11% parent compound and 20 ± 11% THF acetate biomarker). Neither PPIX nor HTF in combination with SA resulted in bioactivation levels that differed significantly from cells treated with either PPIX or HTF alone.

DISCUSSION

Artemisinin and its derivatives are an important class of antimalarial agents that are widely used despite reports of embryotoxicity and neurotoxicity in animal models (3, 4). The

TABLE 3

The effect of modulators of cellular heme biosynthesis and iron content on the cytotoxicity of the ARTs against HL-60 cells (24 h)

The IC_{50} values (μM) were derived from the MTT assay, and heme content was measured by fluorometric detection. All of the results are expressed as the means ± S.D. calculated from four independent experiments. The *p* values indicate the significance of the IC_{50} values and heme content levels for incubations containing ARTs alone compared with those of incubations containing additionally chemical modulators as tested by Student's *t* test for parametric data. NS, non-significant; *, $p < 0.05$; **, $p < 0.01$; ***, $p < 0.001$.

	Artesunate		PFDHA		Heme	
	IC_{50} value	*p* value	IC_{50} value	*p* value	Content	*p* value
	μM		μM		ng/10^6cell	
Cells only					15.4 ± 6.0	
ARTs alone	3.05 ± 1.63		0.36 ± 0.20			
+ SA	55.47 ± 4.65	***	>100		2.8 ± 2.5	**
+ PPIX	0.49 ± 0.27	*	0.12 ± 0.06	**	40.1 ± 26.8	***
+ PPIX + SA	0.88 ± 0.71	*	1.20 ± 0.90	NS	42.2 ± 34.4	**
+ HTF	3.66 ± 1.45	NS	0.36 ± 0.26	NS	17.6 ± 12.2	*
+ HTF + SA	46.09 ± 9.32	***	47.1 ± 23.9	**	16.2 ± 12.7	NS

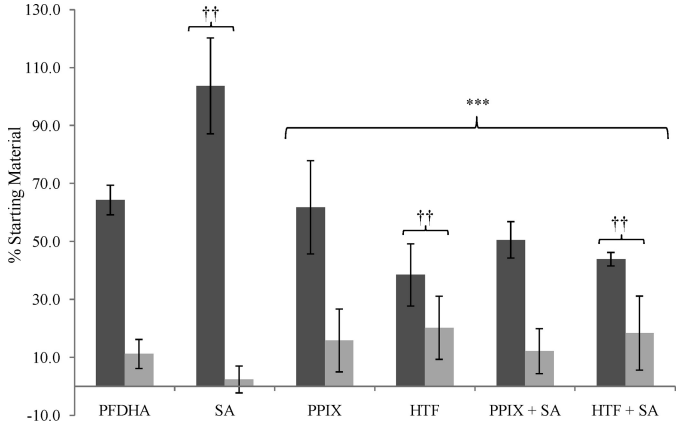

FIGURE 6. **PFDHA (3) activation to PFDHA THF acetate (4) in HL-60 cells is dependent upon cellular heme and iron levels.** The cells were extracted following incubation with PFDHA (1 μM, 24 h) in the presence of various modulators of heme biosynthesis and cellular iron levels: SA (0.5 mM), PPIX (1 μM), and HTF (10 μM) as described under "Experimental Procedures." The amounts of **3** and **4** present were quantified by LC-MS/MS-MRM as described under "Experimental Procedures." *Darker bars*, HeLa cells; *lighter bars*, HeLa ρ^0. The results are the means ± S.D. of four independent sets of experiments. ††, $p < 0.01$ significance of data compared with PFDHA-alone data. ***, $p < 0.001$ significance data compared PFDHA + SA data.

cytotoxic activity of the ARTs against certain mammalian cell lines is well documented, and it is known that the endoperoxide group functions as both a pharmacophore and a toxicophore (11). Despite this shared chemical basis of toxicity and parasiticidal activity, the benefit to risk ratio of the ARTs is high. However, definition of the chemical and molecular mechanisms underlying cytotoxicity against mammalian cells is required to continue their safe use and development. In the present study, we have defined more clearly the mechanism of cell death with respect to molecular activators and the target organelle. We have shown that the mitochondria play an essential role in cytotoxicity; bioactivation of the endoperoxide group must be induced by cellular heme to result in cell death, and subsequent apoptosis is dependent upon reactive oxygen species generation via the activity of the ETC (Fig. 7).

Recent research has suggested that the activity of the ETC may be partially responsible for the reductive activation of the endoperoxide bridge of ARTs to toxic carbon-centered radicals and that these species act locally to induce ROS generation, mitochondria dysfunction, and eventually death (27, 28). Differences in studies of isolated mitochondria from malaria parasites and CHO cells led the authors to hypothesize that this mechanism is specific to the parasite (27). It is important to note that the isolated mitochondria from CHO cells were treated with 100 nM artemisinin, whereas previous studies reported that CHO cells have low sensitivity to the ARTs (artesunate IC_{50} value >130 μM against CHO-9 cells), and therefore this concentration may be too low (40). However, the hypothesis that activation of the endoperoxide group is chemically mediated by the mitochondria remains untested. Therefore, we have used HeLa ρ^0 cells, which lack a functioning ETC to test the role of the ETC in the chemical induction of toxicity in whole cells (34, 41). HeLa cells are sensitive to endoperoxide cytotoxicity (18) and thereby are a relevant system to assess specific mechanisms of ART-induced cell death. These studies have demonstrated that although cells without a functional ETC are significantly less susceptible to ART-induced cell death, cytotoxicity is still evident at high concentrations. This indicates that the molecular components of the ETC encoded by mitochondrial DNA are not the sole target(s) of the ARTs because in their absence cell death is still induced. Quantitative LC-MS/MS-MRM analysis demonstrated that the loss of parent endoperoxide and formation of THF acetate, a biomarker of carbon-centered radical production (17), were the same in each cell line and thus that the same extents of bioactivation took place. Therefore, differential one-electron reduction of the endoperoxide group is not the basis for the measured differences in cytotoxicity between HeLa and HeLa ρ^0 cells, and the ETC plays no role in this activation, in contrast to the original hypothesis presented by the Wang group (27, 28).

It has been widely assumed that a cellular Fe(II) source is responsible for the activation of the endoperoxide functionality; iron chelators and spin traps can reduce both the pharmacological and cytotoxic activity of the endoperoxides (11, 18, 42, 43). Zhang and Gerhard (22) have used heme precursors and an inhibitor of heme synthesis in MOLT-4 leukemia cells to demonstrate the importance of cellular heme in endoperoxide-induced cytotoxicity. In addition they used a biomimetic technique to assess the chemical interaction of artemisinin with heme and concluded that heme could be a target of the ARTs and a physiological mediator of endoperoxide-induced cytotoxicity. However, although the interaction of heme with ARTs has been well characterized using chemical techniques (22, 44, 45), the role of heme in the intracellular

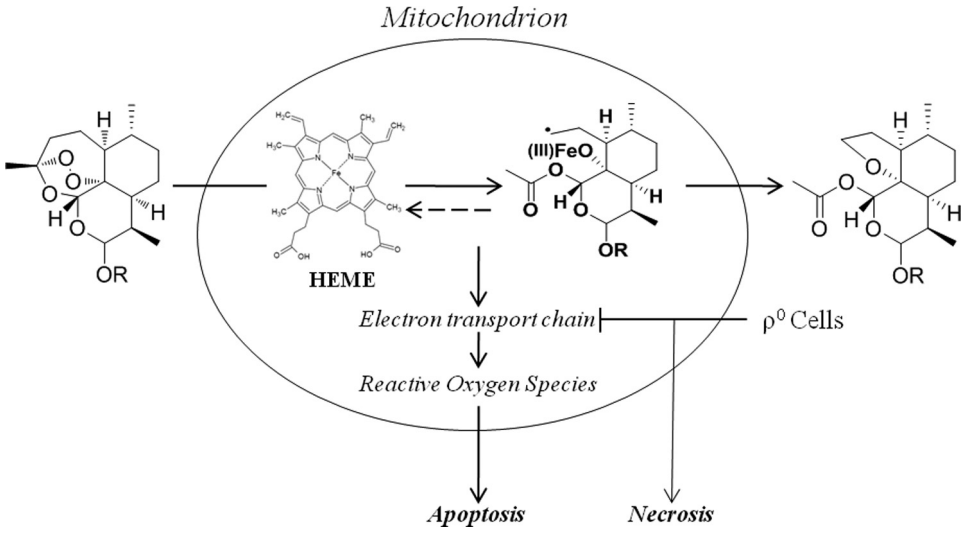

FIGURE 7. **Proposed chemical and molecular pathways of endoperoxide-induced cytotoxicity.**

activation of the endoperoxide group has not been defined. In our studies, we have used several modulators of heme synthesis and intracellular iron content (Fig. 5) to characterize the effects of heme on cell death and endoperoxide activation. SA induced a significant reduction in cellular heme levels that was associated with consistent inhibition of toxicity and diminished activation of the endoperoxide to the THF acetate biomarker. In addition PPIX was shown to increase heme content, which resulted in increased cytotoxicity alongside enhanced endoperoxide bioactivation. Concordantly, when added with SA, PPIX overcame both the inhibition of cytotoxicity and bioactivation of the endoperoxide group because of the restoration of cellular heme levels at a point of the pathway downstream from SA inhibition (Fig. 5). Therefore, this demonstrates that the intracellular bioactivation of the endoperoxide to carbon-centered radicals is dependent upon cellular heme, and moreover, we can confirm that this is the chemical basis of cytotoxicity.

The inhibitory effect of iron chelators upon cytotoxicity and anti-parasitic activity has led researchers to speculate that non-heme, chelatable iron could be responsible for endoperoxide activation (42). However, in our studies, the addition of HTF did not increase cytotoxicity, contrary to the work of others with leukemia and astrocytoma cell lines (43, 46), but LC-MS/MS-MRM quantification did demonstrate a significant increase in the bioactivation of PFDHA. These results indicate that the Fe(II) species contained in HTF is initiating nonspecific endoperoxide activation but that if bioactivation is not specifically mediated by heme, then cell death is not induced. This hypothesis is strengthened by the finding that the addition of HTF with SA only partially restores cytotoxic activity, despite the large increase in bioactivation of the endoperoxide group and the presence of cellular heme, because we postulate that nonspecific HTF-mediated bioactivation acts as a detoxification process that results in reduced levels of ARTs available to interact with cellular targets. These results highlight the importance of the specific location of endoperoxide activation and that bioactivation may need to take place in close proximity to the cellular target. Thus, this evidence, when combined with biomimetic studies demonstrating the ability of the ARTs to alkylate and form adducts with heme, suggests that a heme species may also be a target of the endoperoxides (47, 48). It is of note that the majority of the heme biosynthetic pathway, including the final step, which produces the heme porphyrin, takes place within the mitochondria (39). We therefore hypothesize that heme-dependent endoperoxide activation takes place in the mitochondria and that heme-dependent bioactivation is the chemical basis for the importance of the mitochondria in endoperoxide-induced cell death. Furthermore, the reduced sensitivity of ρ^0 cells may be a consequence of the absence of an active ETC, which depends on several heme-containing proteins to function (49).

The differential toxicity displayed by the ρ^+/ρ^0 model was further examined to gain a better understanding of the molecular basis of cell death. The role of ROS generation during endoperoxide-induced cytotoxicity is controversial (18, 19). However, these reported differences may arise because of variations in experimental protocols and the transient nature of ROS. During this study, the cells were pretreated with DCFH-DA, and early ROS generation (16 h) was observed. This early onset of ROS generation before cytotoxicity is detected (48 h) suggests that it is an initiating event in cytotoxicity. The reduced ROS levels measured in HeLa ρ^0 cells indicate that the ETC is involved in their generation, which is supported by the well characterized role of the ETC in the induction of ROS (50). However, the induction of ROS and antioxidant defense mechanisms in ρ^0 cells is a complex area, and so these results must be interpreted with caution (51–53). The role of ROS generation in the initiation of cell death was confirmed using tiron, a cell-permeable superoxide scavenger (38) that inhibited ROS generation and abrogated subsequent cell death. These findings demonstrate that artesunate-induced ROS generation is a consequence of ETC activity and is an important initiating event in the induction of apoptotic cell death.

In agreement with a previous study, in our investigations artesunate induced apoptotic cell death in HeLa cells via mi-

tochondrial membrane depolarization, cytochrome *c* release, and caspase-3/7 activity (18), but the mechanism of cell death in HeLa ρ^0 cells was more complex. Annexin V/propidium iodide staining demonstrated that artesunate induced predominantly necrotic cell death, with only low levels of apoptosis observed, and this was further confirmed by reduced mitochondrial depolarization, cytochrome *c* release, and a lack of caspase-3/7 activation in these cells.

Overall these results indicate that multiple target(s) and/or pathways of artesunate cell death exist but that without ROS generation, the toxicity levels are significantly reduced, and therefore this is the primary mechanism of cell death. It is clear that concomitant ROS-independent pathways have the ability to induce cell death, although from these studies it is unclear whether these pathways directly induce necrosis or whether this is a consequence of the inability of the HeLa ρ^0 cells to undergo full apoptosis. Although it has been shown that the lack of a functioning ETC does not fundamentally impair the ability of a cell to undergo mitochondria-mediated apoptosis (54), cell death is extremely stimulus-dependent, and so these results require further consideration. Apoptosis is an active program that requires ATP, and necrosis is initiated if a cell does not have sufficient energy to carry out apoptosis (55). Although in this case both cell lines have comparable base-line ATP levels (HeLa, 110 ± 14 nmol of ATP/10^6 cells; and HeLa ρ^0, 99 ± 8 nmol of ATP/10^6 cells; data not shown), initial apoptotic cell death can be switched to necrosis if HeLa ρ^0 cells are unable to generate further ATP, because of the absence of the ETC, to support ongoing apoptosis. This hypothesis would account for the initial low levels of mitochondrial depolarization, and cytochrome *c* release induced by artesunate before energy shortages causes necrotic cell death to predominate. This switch in cell death in HeLa ρ^0 cells caused by ATP shortages, despite initial high levels, has been described (56). In addition, the differential activation of apoptosis and necrosis by dihydroartemisinin in different cell types has recently been reported (57). In this publication necrosis was observed in dihydroartemisinin-treated primary lymphocytes isolated from patients with chronic lymphocytic leukemia, which are known to have defective apoptotic machinery.

In conclusion, these studies have advanced our understanding of the chemical and molecular mechanisms of endoperoxide-induced cell death. We have demonstrated that endoperoxide bioactivation to carbon-centered radicals only results in cytotoxicity when it is mediated by heme or a heme-containing protein. We hypothesize that these radicals then act locally within the mitochondria to modify heme or heme-containing proteins, which results in the generation of ROS via ETC dysfunction and the induction of cell death via apoptosis (Fig. 7). This work presents a unified chemical rationale for the sensitivity of cancer cells that have up-regulated iron metabolism and heme synthesis to maintain continuous growth and proliferation (21) and to primitive erythroblasts, defined as the embryotoxic target of the ARTs (58), which have active mitochondria and heme synthesis.

REFERENCES

1. Nosten, F., and White, N. J. (2007) *Am. J. Trop. Med. Hyg.* **77,** 181–192
2. Park, B. K., O'Neill, P. M., Maggs, J. L., and Pirmohamed, M. (1998) *Br. J. Clin. Pharmacol.* **46,** 521–529
3. Clark, R. L., White, T. E., Clode, S. A., Gaunt, I., Winstanley, P., and Ward, S. A. (2004) *Birth Defects Res. B Dev. Reprod. Toxicol.* **71,** 380–394
4. Toovey, S. (2006) *Toxicol. Lett.* **166,** 95–104
5. Clark, R. L. (2009) *Reprod. Toxicol.* **28,** 285–296
6. World Health Organization (2003) *WHO/CDS/MAL/2003.1094*
7. Muller, O., Sie, A., Meissner, P., Schirmer, R. H., and Kouyate, B. (2009) *Lancet* **374,** 1419–1419
8. Taylor, S. M., Juliano, J. J., and Meshnick, S. R. (2009) *N. Engl. J. Med.* **361,** 1807–1807
9. Noedl, H., Se, Y., Schaecher, K., Smith, B. L., Socheat, D., Fukuda, M. M., and Consortium, A. S. (2008) *N. Engl. J. Med.* **359,** 2619–2620
10. Jefford, C. W. (2007) *Drug Discovery Today* **12,** 487–495
11. Mercer, A. E. (2009) *Curr. Opin. Drug Discovery Dev.* **12,** 125–132
12. Posner, G. H., D'Angelo, J., O'Neill, P. M., and Mercer, A. (2006) *Exp. Opin. Therapeutic Patents* **16,** 1665–1672
13. O'Neill, P. M., and Posner, G. H. (2004) *J. Med. Chem.* **47,** 2945–2964
14. Eckstein-Ludwig, U., Webb, R. J., Van Goethem, I. D., East, J. M., Lee, A. G., Kimura, M., O'Neill, P. M., Bray, P. G., Ward, S. A., and Krishna, S. (2003) *Nature* **424,** 957–961
15. Berman, P. A., and Adams, P. A. (1997) *Free Radic. Biol. Med.* **22,** 1283–1288
16. Robert, A., Benoit-Vical, F., Claparols, C., and Meunier, B. (2005) *Proc. Natl. Acad. Sci. U.S.A.* **102,** 13676–13680
17. Mercer, A. E., Maggs, J. L., Sun, X. M., Cohen, G. M., Chadwick, J., O'Neill, P. M., and Park, B. K. (2007) *J. Biol. Chem.* **282,** 9372–9382
18. Disbrow, G. L., Baege, A. C., Kierpiec, K. A., Yuan, H., Centeno, J. A., Thibodeaux, C. A., Hartmann, D., and Schlegel, R. (2005) *Cancer Res.* **65,** 10854–10861
19. Lu, J. J., Meng, L. H., Cai, Y. J., Chen, Q., Tong, L. J., Lin, L. P., and Ding, J. (2008) *Cancer Biol. Ther.* **7,** 1017–1023
20. Efferth, T., Dunstan, H., Sauerbrey, A., Miyachi, H., and Chitambar, C. R. (2001) *Int. J. Oncol.* **18,** 767–773
21. Kwok, J. C., and Richardson, D. R. (2002) *Crit. Rev. Oncol. Hematol.* **42,** 65–78
22. Zhang, S. M., and Gerhard, G. S. (2009) *PLoS One* **4,** e7472
23. Jiang, J. B., Jacobs, G., Liang, D. S., and Aikawa, M. (1985) *Am. J. Trop. Med. Hyg.* **34,** 424–428
24. Maeno, Y., Toyoshima, T., Fujioka, H., Ito, Y., Meshnick, S. R., Benakis, A., Milhous, W. K., and Aikawa, M. (1993) *Am. J. Trop. Med. Hyg.* **49,** 485–491
25. Longo, M., Zanoncelli, S., Della Torre, P., Rosa, F., Giusti, A., Colombo, P., Brughera, M., Mazué, G., and Olliaro, P. (2008) *Reprod. Toxicol.* **25,** 433–441
26. Laffan, S. B., James, A. C., Maleeff, B. E., Pagana, J. M., Clark, R. L., and White, T. E. (2006) *Birth Defects Res. A Clin. Mol. Teratol.* **76,** 329–329
27. Wang, J., Huang, L., Li, J., Fan, Q., Long, Y., Li, Y., and Zhou, B. (2010) *PLoS One* **5,** e9582
28. Li, W., Mo, W. K., Shen, D., Sun, L. B., Wang, J., Lu, S., Gitschier, J. M., and Zhou, B. (2005) *PLoS Genet.* **1,** 329–334
29. O'Neill, P. M., Miller, A., Bishop, L. P., Hindley, S., Maggs, J. L., Ward, S. A., Roberts, S. M., Scheinmann, F., Stachulski, A. V., Posner, G. H., and Park, B. K. (2001) *J. Med. Chem.* **44,** 58–68
30. Tennant, J. R. (1964) *Transplantation* **2,** 685–694
31. Repetto, G., del Peso, A., and Zurita, J. L. (2008) *Nat. Protoc.* **3,** 1125–1131
32. Mercer, A. E., Regan, S. L., Hirst, C. M., Graham, E. E., Antoine, D. J., Benson, C. A., Williams, D. P., Foster, J., Kenna, J. G., and Park, B. K. (2009) *Toxicol. Appl. Pharmacol.* **239,** 297–305
33. Sassa, S. (1976) *J. Exp. Med.* **143,** 305–315
34. Rodríguez-Enríquez, S., Vital-González, P. A., Flores-Rodríguez, F. L., Marín-Hernández, A., Ruiz-Azuara, L., and Moreno-Sánchez, R. (2006)

Toxicol. Appl. Pharmacol. **215,** 208–217
35. King, M. P., and Attardi, G. (1989) *Science* **246,** 500–503
36. Berridge, M. V., and Tan, A. S. (1998) *Protoplasma* **205,** 74–82
37. Green, D. R., and Reed, J. C. (1998) *Science* **281,** 1309–1312
38. Greenstock, C. L., and Miller, R. W. (1975) *Biochim. Biophys. Acta* **396,** 11–16
39. Ponka, P. (1997) *Blood* **89,** 1–25
40. Li, P. C., Lam, E., Roos, W. P., Zdzienicka, M. Z., Kaina, B., and Efferth, T. (2008) *Cancer Res.* **68,** 4347–4351
41. Nass, M. M. (1970) *Proc. Natl. Acad. Sci. U.S.A.* **67,** 1926–1933
42. Stocks, P. A., Bray, P. G., Barton, V. E., Al-Helal, M., Jones, M., Araujo, N. C., Gibbons, P., Ward, S. A., Hughes, R. H., Biagini, G. A., Davies, J., Amewu, R., Mercer, A. E., Ellis, G., and O'Neill, P. M. (2007) *Angew. Chem. Int. Ed. Engl.* **46,** 6278–6283
43. Efferth, T., Benakis, A., Romero, M. R., Tomicic, M., Rauh, R., Steinbach, D., Häfer, R., Stamminger, T., Oesch, F., Kaina, B., and Marschall, M. (2004) *Free Radic. Biol. Med.* **37,** 998–1009
44. Zhang, S., and Gerhard, G. S. (2008) *Bioorg. Med. Chem.* **16,** 7853–7861
45. Cazelles, J., Robert, A., and Meunier, B. (2002) *J. Org. Chem.* **67,** 609–619
46. Singh, N. P., and Lai, H. C. (2004) *Anticancer Res.* **24,** 2277–2280
47. Robert, A., Coppel, Y., and Meunier, B. (2002) *Chem. Commun.* 414–415
48. Zhang, S., and Gerhard, G. S. (2009) *PLoS One* **4,** e7472
49. Atamna, H., Walter, P. B., and Ames, B. N. (2002) *Arch. Biochem. Biophys.* **397,** 345–353
50. Andreyev, A. Y., Kushnareva, Y. E., and Starkov, A. A. (2005) *Biochemistry-Moscow* **70,** 200–214
51. Vergani, L., Floreani, M., Russell, A., Ceccon, M., Napoli, E., Cabrelle, A., Valente, L., Bragantini, F., Leger, B., and Dabbeni-Sala, F. (2004) *Eur. J. Biochem.* **271,** 3646–3656
52. Ferraresi, R., Troiano, L., Pinti, M., Roat, E., Lugli, E., Quaglino, D., Taverna, D., Bellizzi, D., Passarino, G., and Cossarizza, A. (2008) *Cytometry* **73,** 528–537
53. Park, S. Y., Chang, I., Kim, J. Y., Kang, S. W., Park, S. H., Singh, K., and Lee, M. S. (2004) *J. Biol. Chem.* **279,** 7512–7520
54. Jiang, S., Cai, J., Wallace, D. C., and Jones, D. P. (1999) *J. Biol. Chem.* **274,** 29905–29911
55. Nicotera, P., Leist, M., and Ferrando-May, E. (1998) *Toxicol. Lett.* **103,** 139–142
56. Miyoshi, N., Watanabe, E., Osawa, T., Okuhira, M., Murata, Y., Ohshima, H., and Nakamura, Y. (2008) *Biochim. Biophys. Acta* **1782,** 566–573
57. Handrick, R., Ontikatze, T., Bauer, K. D., Freier, F., Rübel, A., Dürig, J., Belka, C., and Jendrossek, V. (2010) *Mol. Cancer Ther.* **9,** 2497–2510
58. Longo, M., Zanoncelli, S., Torre, P. D., Riflettuto, M., Cocco, F., Pesenti, M., Giusti, A., Colombo, P., Brughera, M., Mazué, G., Navaratman, V., Gomes, M., and Olliaro, P. (2006) *Reprod. Toxicol.* **22,** 797–810